JOURNAL OF AIRCRAFT
Vol. 42, No. 1, January–February 2005

Nonlinear Aerodynamic Model Extraction from Flight-Test Data for the S-3B Viking

Alfonso C. Paris* and Omeed Alaverdi†
Science Applications International Corporation, Lexington Park, Maryland 20653

Applied procedures for nonlinear aerodynamic model development and extraction from flight data for the S-3B Viking aircraft are addressed. The entire analysis procedure, from dynamic flight-test data management to final blending and validation of the upgraded aerodynamic model, was performed within the integrated data evaluation and analysis system developed by Science Applications International Corporation. A variety of parameter identification (PID) techniques were employed to develop a global, fully nonlinear longitudinal and lateral–directional aerodynamic model. This effort included total aerodynamic coefficient reconstruction, equation error analysis for initial model structure development, and output error analysis for final model tuning. Data available from S-3B PID flight spanned a Mach range of 0.23–0.60 which covered an adequate range of angle of attack for both nonlinear longitudinal and lateral–directional analyses. Regions outside the identified model envelope were described by blending with the original S-3B aerodynamic database to create a full envelope model. Aircraft configurations investigated included cruise, maneuver, takeoff, and landing flap settings as well as retracted and extended landing gear. Standard flight-test maneuvers were flown under each configuration and are described. The available data allowed for the successful extraction of component coefficients for aircraft lift, side force, pitching, rolling, and yawing moments resulting in a simulation with high aerodynamic fidelity.

Nomenclature

$\boldsymbol{A}$	=	regressor matrix
$\boldsymbol{A}_s$	=	thinned regressor matrix
b	=	wing span
C_l	=	aerodynamic rolling moment coefficient
C_m	=	aerodynamic pitching moment coefficient
C_n	=	aerodynamic yawing moment coefficient
$\bar{c}$	=	mean aerodynamic chord
F	=	Athena fit percentage
f	=	spline basis function
M	=	Mach number
N	=	total number of residual vector elements
p, q, r	=	body axis roll, pitch, and yaw angular rates
$\boldsymbol{p}$	=	final parameter vector
$\boldsymbol{p}_s$	=	incremental parameter vector
$\boldsymbol{p}_0$	=	a priori parameter vector
$\boldsymbol{S}$	=	singular value diagonal matrix
U	=	Theil statistic
U_b, U_c, U_v	=	Theil statistic bias, covariance, and variance proportions
V	=	airframe velocity
$\boldsymbol{v}$	=	system/sensor noise vector
y	=	measured airframe response
$\boldsymbol{y}$	=	nondimensional force/moment coefficient vector
$\boldsymbol{y}_s$	=	incremental nondimensional force/moment coefficient vector
$\hat{y}$	=	simulation predicted airframe response
α	=	angle of attack
$\dot{\alpha}$	=	angle-of-attack rate
β	=	angle of sideslip
δ_a	=	aileron deflection
δ_e	=	elevator deflection
δ_{et}	=	elevator tab deflection
δ_F	=	flap deflection
δ_H	=	horizontal stabilator deflection
δ_{LG}	=	landing gear extension, 1 = full extension and 0 = full retraction
δ_r	=	rudder deflection
δ_{sp}	=	spoiler deflection
δ_{tr}	=	rudder trim deflection
ρ	=	correlation coefficient
Σ	=	summation
σ	=	standard deviation

Superscripts

T	=	transpose
$+$	=	pseudoinverse

Presented as Paper 2001-4015 at the AIAA AFM conference proceedings held in Montreal, Canada, 6–9 August 2001; received 17 June 2003; revision received 5 November 2003; accepted for publication 7 November 2003.

*Aerospace Engineer, Simulation and Research Services Division, 22299 Exploration Drive, Suite 200; alfonso.paris@saic.com. Member AIAA.

†Chief Engineer, Simulation and Research Services Division, 22299 Exploration Drive, Suite 200; omeed.alaverdi@saic.com. Member AIAA.

Introduction

THE S-3B is a high-wing, twin engine U.S. Navy aircraft produced by Lockheed Martin. It has been in service since 1974. Current S-3B flight simulator models have been shown to be insufficient for pilot training in such tasks as aerial refueling, field and carrier approaches, and landings.[1] Consequently, Science Applications International Corporation (SAIC) was involved in an overall aerodynamic model simulation upgrade for the S-3B operational flight trainer (OFT) with the final goal of increasing model fidelity in the aforementioned flight regimes. Although not outlined in detail within this paper, SAIC was also responsible for additional upgrades in this program regarding the TF-34 engine model, aircraft weight and balance formulation, and appropriate implementation of aircraft equations of motion and atmospheric models. Flights performed in the summer of 1996 at the Naval Air Warfare Center, Aircraft Division, Patuxent River, Maryland resulted in a wealth of flight-test data appropriate for PID purposes.

The integrated data evaluation and analysis system (IDEAS) is a powerful database management system and analysis software containing a full complement of flight data preprocessing, calibration, simulation, model estimation, model verification, and validation tools.[2,3] This analysis package, developed by SAIC, was used extensively in support of the S-3B OFT simulation update.

Flight-test data collected for the purpose of aerodynamic parameter estimation typically consists of inertial and air-relative sensor outputs. Before parameter estimation, or traditional data reduction was performed, it was necessary to evaluate and correct the measured data to ensure kinematic consistency of the inertial sensors, as well as accuracy of the critical air-relative parameters. Consequently, a rigorous postflight data calibration study was performed within IDEAS. Resulting corrections, in the form of biases and/or scale factors, were applied to the appropriate inertial and air-data sensors to arrive at a consistent set of data suitable for PID purposes.[4]

Additional data preprocessing resulted in overall aircraft weight and balance, as well as engine thrust information, for each PID maneuver. Given this information, tools within IDEAS allowed for the extraction of total aerodynamic force and moment coefficient histories for each PID maneuver.

Test data from maneuvers of comparable configuration were placed into analysis groups with ample data made available to span a suitable range of the flight-test envelope. Initial aerodynamic model structures were developed through analysis of these groups using an equation error extraction technique in IDEAS known as Athena. Athena expresses the overall aerodynamic forces and moments as linear combinations of stability derivatives and/or increments. In addition, the capabilities of Athena allow for such terms to be modeled with nonlinear functionalities by employing basis spline functions. The resulting model was installed in a simulation for the S-3B airframe within IDEAS to be used in further PID studies.

This newly developed aerodynamic model was further adjusted through estimation of increments to appropriate coefficients using an output error technique. This step was necessary to deal appropriately with any estimate biases that may have resulted from the equation error procedure. Within IDEAS, this technique involves the use of a nonlinear least-squares optimization algorithm known as LSIDNT coupled with a version of the S-3B airframe simulation containing the aerodynamic upgrade identified using Athena.

The final identified model was blended with the baseline S-3B aerodynamic data package to result in a full envelope model on which validation studies were performed. An overview of the model development process is shown in Fig. 1.

Overall, PID analysis resulted in updates for both model structure and aerodynamic coefficients of lift and side force as well as pitching, rolling, and yawing moment coefficients. The upgraded model retains the thrust and drag performance parameters measured, and provided, by the Flight Vehicle Simulation Branch of the Naval Air Systems Command.[5,6]

Each of the total aerodynamic coefficients follows a similar basic structure in that they consist of a sum of incremental effects. These contributions include effects due to a basic, or bias, aerodynamic coefficient, air-relative orientation, aircraft stability axis angular rates, control surface positions, and weapon stores.

The following sections examine the required data preprocessing, model structure development, and aerodynamic model extraction techniques in detail.

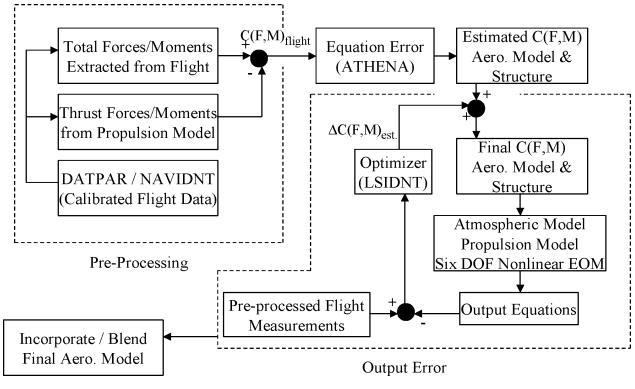

Fig. 1 Aerodynamic model development process using both equation error and output error.

Available Flight-Test Maneuvers

Standard PID maneuvers were chosen from the S-3B dynamic flight-test database for the purpose of aerodynamic model extraction. Maneuvers examined include pilot-applied all-axis control doublets, all-axis control 3–2–1–1s, bank-to-bank aileron/spoiler rolls, and bank-to-bank aileron rolls. These maneuver classes were performed in blocks at each aircraft configuration investigated including (listed in order of increasing flap deflection) cruise, maneuver, takeoff, and landing flap settings as well as retracted and extended landing gear. All maneuvers were flown with wing pylons in place and no additional external loads. Each maneuver block contained the following maneuvers, flown back-to-back, for each flight condition and aircraft configuration: 360-deg coordinated heading change turn, longitudinal stick doublet, longitudinal stick 3–2–1–1, lateral stick doublet (aileron/spoiler interconnect active), lateral stick 3–2–1–1 (aileron/spoiler interconnect active), directional pedal doublet, directional pedal 3–2–1–1, lateral stick bank-to-bank roll attitude capture (aileron/spoiler interconnect active), and lateral stick bank-to-bank roll attitude capture (aileron only).

The coordinated heading change turn that precedes each block of PID maneuvers was instrumental in the data calibration process because it provided valuable information regarding the magnitude and direction of atmospheric winds.[4] However, they were not analyzed during the PID process because they did not contain adequate mode excitation. The stick/pedal doublets and 3–2–1–1s were designed to excite the aircraft short period and Dutch roll modes appropriately. The lateral stick bank-to-bank roll attitude captures were flown with both the aileron/spoiler interconnect active as well as inactive (aileron excitation only). This provided valuable information allowing for the differentiation between aileron and spoiler roll control/adverse yaw power.

A total of 56 individual PID maneuvers were separated into a series of five longitudinal and five lateral–directional analysis groups within IDEAS. Each group contained a collection of appropriate maneuvers from the preceding list that were flown under identical aircraft configuration. The configurations represented by the analysis groups are cruise flap setting/landing gear up, cruise flap setting/landing gear down, maneuver flap setting/landing gear up, takeoff flap setting/landing gear down, and landing flap setting/landing gear down. Such analysis groups are instrumental during the PID process in that they present a wealth of information, via a collection of PID maneuvers, to the estimation algorithm allowing for the extraction of a global aerodynamic model.

Dynamic Flight-Test Data Preprocessing

Previous studies within IDEAS examined pertinent channels from each maneuver for data dropouts and/or signal wrapping. Appropriate tools within the IDEAS data preprocessing and reconstruction (DATPAR) toolbox were employed to correct such anomalies when they occurred.[2,3]

In addition, previous extensive calibration studies within IDEAS resulted in inertial and air-data sensor adjustments, in the form of biases and/or scale factors, applied to the appropriate flight data to develop a set of consistent data.[4]

Finally, DATPAR tools were used to compute a variety of important histories for each maneuver including stability axis angular rates, dynamic pressure, ambient temperature, true airspeed, Mach, air relative velocities, air relative body axis accelerations, and angular accelerations.

Total Aerodynamic Force and Moment Extraction

A variety of data is necessary to extract successfully total aerodynamic force and moment coefficients from flight data. These data consist of body axis angular rates and accelerations, body axis linear accelerations, dynamic pressure, and body axis thrust produced forces and moments, as well as aircraft mass and inertia data. In addition, to facilitate transferring the overall moments to a specific reference point, about which the aerodynamic model is to be developed, the center of gravity location for each maneuver must be determined.

Appropriate angular rate, angular acceleration, linear acceleration, and dynamic pressure data were acquired during DATPAR preprocessing as outlined in the preceding section. Suitable information regarding aircraft mass characteristics as well as body axis thrust forces and moments had to be determined.

To complete this task, the baseline S-3B OFT airframe model was installed as a simulation running within the IDEAS environment. This development version of the OFT airframe included a new weight and balance module updated by SAIC to model more accurately the S-3B experimental loading.[7] Aerodynamic model updates resulting from this work would later be applied to this version of the simulation.

Characteristics such as aircraft mass, center-of-gravity position, and inertias were acquired by running the developmental OFT airframe simulation within the IDEAS environment. Appropriate loading conditions (fuel, stores, etc.) were set as per each individual PID maneuver to be employed for model development. This process involved trimming the simulation at the initial conditions per maneuver and overriding the surface positions with flight-recorded control deflections during run time. The initial baseline simulation runs provided a preliminary look into the strengths and weaknesses of the original OFT aerodynamic model by allowing a comparison between simulated and recorded aircraft responses. Predicted aircraft weight and balance information was also saved within the IDEAS database for each PID maneuver investigated.

Similarly, thrust body axis forces and moments for each maneuver were determined by running a stand-alone upgraded simulation of the TF-34 engines within the IDEAS environment.[8] In this case, quantities such as pressure and inertial altitude, ambient temperature, reconstructed true airspeed, and engine fan speeds were overridden within the simulation using preprocessed and recorded flight data. Resulting thrust forces and moments were saved within the IDEAS database. The upgraded engine model was later incorporated into the final developmental S-3B OFT airframe simulation.

With all necessary data made available to extract the total aerodynamic moment and force coefficients, a variety of IDEAS tools were employed, which resulted in overall aerodynamic lift, drag, side force, pitching moment, rolling moment, and yawing moment coefficient histories with respect to the aircraft c.g. per PID maneuver.[2,3] All body axis total force coefficients were reconstructed assuming a rigid-body aircraft with negligible effects due to spinning engine rotors.

Additional IDEAS tools were used to transfer all reconstructed body axis aerodynamic moments to the desired reference point about which the aerodynamic model would be developed.[2,3] This transference involves the incremental effects due to the reconstructed body axis aerodynamic forces about the aircraft c.g. being offset from the desired aerodynamic reference center. Because the baseline S-3 OFT aerodynamic model was defined about the stability axis, the corresponding aerodynamic coefficients were transferred about that axis system.

Aerodynamic Model Structure Development Using Equation Error

Estimation Algorithm

The next stage of analysis involved an equation error PID technique to extract a new set of aerodynamic stability derivatives for the S-3B. The equation error tool in IDEAS, known as Athena, is capable of determining the overall aerodynamic force and moment models as linear combinations of parameters (typically stability derivatives and/or incremental coefficients) by the use of a principal component regression algorithm.[2,3,9,10] In addition, Athena allows these terms to be modeled with nonlinear dependencies. As an example, consider a very simple pitching moment buildup,

$$C_m = C_{m\text{basic}}(\alpha) + C_{m\delta e}(\alpha)\cdot\delta_e \tag{1}$$

In this example the overall model structure is a nonlinear function of angle of attack. To model the nonlinearities, Athena supports the use of linear or cubic basis splines to estimate linear coefficients of the splines at the specified knot locations of the nonlinear function. Equation (1) is rewritten as

$$C_m = \sum_{i=1}^{K1} C_{m\text{basic},i}\cdot f_{1,i}(\alpha) + \sum_{i=1}^{K2} C_{m\delta e,i}\cdot f_{2,i}(\alpha)\cdot\delta_e \tag{2}$$

$C_{m\text{basic},i}$ and $C_{m\delta e,i}$ are the parameters to be estimated; $K1$ and $K2$ are the number of angle-of-attack knot locations defined for $C_{m\text{basic}}$ and $C_{m\delta e}$, respectively; and $f_{1,i}(\alpha)$ and $f_{2,i}(\alpha)$ are basis functions. Typically, the basis functions are defined such that each takes on a value of 1.0 at one knot location and a value of 0.0 at all other knot locations.

Athena assumes the model may be represented as a set of linearly combined, time-independent linear parameters with the following structure:

$$\boldsymbol{y} = \boldsymbol{A}\boldsymbol{p} + \boldsymbol{v} \tag{3}$$

Vector $\boldsymbol{y}$ (size $n\times 1$) represents the total nondimensional force or moment coefficient history vector under investigation. The parameter vector $\boldsymbol{p}$ (size $m\times 1$) represents the stability and control derivatives under estimation, and the regressor matrix $\boldsymbol{A}$ (size $n\times m$) contains the independent variables. Vector $\boldsymbol{v}$ (size $n\times 1$) represents unmodeled aerodynamic responses and/or phenomena such as due to system/sensor noise. Consider the example outlined by Eqs. (1) and (2) assuming two angle-of-attack knot locations are chosen for both $C_{m\text{basic}}$ and $C_{m\delta e}$. In this case, Eq. (3) becomes

$$\begin{bmatrix} C_m(1) \\ \vdots \\ C_m(n) \end{bmatrix} = \begin{bmatrix} f_{1,1}(\alpha(1)) & f_{1,2}(\alpha(1)) & f_{2,1}(\alpha(1))\cdot\delta_e(1) & f_{2,2}(\alpha(1))\cdot\delta_e(1) \\ \vdots & \vdots & \vdots & \vdots \\ f_{1,1}(\alpha(n)) & f_{1,2}(\alpha(n)) & f_{2,1}(\alpha(n))\cdot\delta_e(n) & f_{2,2}(\alpha(n))\cdot\delta_e(n) \end{bmatrix} \times \begin{bmatrix} C_{m\text{basic},1} \\ C_{m\text{basic},2} \\ C_{m\delta e,1} \\ C_{m\delta e,2} \end{bmatrix} + \begin{bmatrix} v(1) \\ \vdots \\ v(n) \end{bmatrix} \tag{4}$$

Athena uses a numerically robust singular value decomposition method to solve Eq. (3) and estimate the parameter vector $\boldsymbol{p}$. In general, Athena first determines an incremental response vector $\boldsymbol{y}_s$ by removing the prior model contributions $\boldsymbol{p}_0$,

$$\boldsymbol{y}_s = \boldsymbol{y} - \boldsymbol{A}\boldsymbol{p}_0 \tag{5}$$

Vector $\boldsymbol{p}_0$ consists of a priori estimates of parameters, as well as parameters that have been fixed and are not to be estimated. The regressor matrix $\boldsymbol{A}$ is then thinned such that it contains only those columns that correspond to parameters that are to be estimated. The thinned matrix $\boldsymbol{A}_s$ allows the identification statement of Eq. (3) to be reformulated as follows:

$$\boldsymbol{y}_s = \boldsymbol{A}_s\boldsymbol{p}_s + \boldsymbol{v} \tag{6}$$

The thinned regressor matrix $\boldsymbol{A}_s$ is then decomposed into the following form:

$$\boldsymbol{A}_s = \boldsymbol{U}\boldsymbol{S}\boldsymbol{V}^T \tag{7}$$

where $\boldsymbol{U}$ and $\boldsymbol{V}$ are orthogonal and $\boldsymbol{S}$ is a diagonal matrix containing the singular values. When Eqs. (6) and (7) are used together, the free parameters are then estimated in principal component axes,

$$\boldsymbol{p}_s = \boldsymbol{V}\boldsymbol{S}^{+}\boldsymbol{U}^T\boldsymbol{y}_s \tag{8}$$

Note that vectors $\boldsymbol{p}_0$ and $\boldsymbol{p}_s$ are combined to yield the final parameter estimates,

$$\boldsymbol{p} = \boldsymbol{p}_0 + \boldsymbol{p}_s \tag{9}$$

Output statistics for this technique are provided in the form of a fit percentage based on the Theil inequality coefficient statistic U defined as (see Ref. 11)

$$U = \frac{\sqrt{(1/N)\sum_{i=1}^{N}(\hat{y}_i - y_i)^2}}{\sqrt{(1/N)\sum_{i=1}^{N}(\hat{y}_i)^2} + \sqrt{(1/N)\sum_{i=1}^{N}(y_i)^2}} \tag{10}$$

N is the total number of points in the residual vector. This coefficient represents the ratio of the root mean square fit error and the root mean square values of the estimated and actual signal summed together. The value of U always falls between 0 and 1, with 0 indicating a perfect fit and 1 the worst fit.

The Athena fit percentage F, a measure of signal fit quality, is defined as follows:

$$F = 100(1 - U) \tag{11}$$

A 100% fit represents a perfect match with the measured data.

Additionally, Athena breaks the fit error into bias, U_b, variance, U_v, and covariance, U_c, proportions as follows[11]:

$$U_b = \frac{(\bar{\hat{y}} - \bar{y})^2}{(1/N)\sum_{i=1}^{N}(\hat{y}_i - y_i)^2} \tag{12a}$$

$$U_v = \frac{(\sigma_{\hat{y}} - \sigma_y)^2}{(1/N)\sum_{i=1}^{N}(\hat{y}_i - y_i)^2} \tag{12b}$$

$$U_c = \frac{2(1-\rho)\sigma_{\hat{y}}\sigma_y}{(1/N)\sum_{i=1}^{N}(\hat{y}_i - y_i)^2} \tag{12c}$$

where ρ and σ represent the correlation coefficient and standard deviation, respectively.

$$\rho = \frac{1}{\sigma_y \sigma_{\hat{y}} N}\sum_{i=1}^{N}(\hat{y}_i - \bar{\hat{y}})(y_i - \bar{y}) \tag{13a}$$

$$\sigma_x = \sqrt{\frac{1}{N}\sum_{i=1}^{N}(x_i - \bar{x})^2} \tag{13b}$$

where $x = y$ or $\hat{y}$.

The bias proportion presents the deviation of the average values of the simulated and measured data acting as a measure of model systematic error. The variance proportion acts as a measure of the model's ability to duplicate the variability in the true system. The covariance proportion is a measure of nonsystematic error. Note that these three proportions sum to 1, with the ideal fit having U_b and U_v close to zero, with U_c close to 1.

These fit statistics act as a measure of accuracy and/or certainty in the proposed model formulation under investigation and provide clues into the effectiveness, or lack thereof, of adjustments introduced in the model structure.

An additional strength of this algorithm is its ability to analyze multiple segments of information, in this case PID maneuvers, simultaneously. This allows for the extraction of global models from analysis groups given multiple PID maneuvers. Overall, this procedure is a fast, single-pass algorithm that results in good base model structure determination.

Algorithm Application

Athena was employed to extract initial parameter estimates for lift, side force, pitching moment, rolling moment, and yawing moment coefficients given the kinematically consistent dynamic flight data and earlier reconstructed aerodynamic total force and moment coefficients. The ability of Athena to estimate nonlinearities in coefficient trends using basis spline functions was exercised by analyzing groupings of PID maneuvers with the goal of determining a global aerodynamic model. Cubic basis splines were utilized in this analysis. Sufficient data spanning a range of Mach and angle of attack were made available to the algorithm providing a wealth of information.

Placement of spline knot locations is crucial in this process. Knots should be placed within regions where sufficient data are available for the breakpoint in question. In this study, knot locations were predominant for aircraft α and Mach throughout all force and moment model buildups. As a result, when analyzing a group of PID maneuvers, knot locations for angle of attack and Mach were distributed evenly such that they fell within appropriate values for the data collectively within that group.

Not only was Athena successful at extracting the basic cruise condition aerodynamic coefficients, but it was also used to estimate incremental effects on the base model parameters due to flap and landing gear deployment. This was accomplished by adding incremental coefficients in the model formulation. Sample aerodynamic moment coefficient structures identified in this work using Athena are as follows:

$$\begin{aligned} C_m = {} & C_{m_o}(M) + C_{m_\alpha}(M)\alpha + C_{m_{\delta_e}}(M)\delta_e + C_{m_{\delta_{e_t}}}(M)\delta_{e_t} \\ & + C_{m_{\delta_H}}(M)\delta_H + C_{m_q}(M)(q\bar{c}/2V) + C_{m_{\dot{\alpha}}}(\dot{\alpha}\bar{c}/2V) \\ & + \Delta C_{m_{o_{\text{pylon}}}} + C_{m_{\delta_F}}\delta_F + \left(C_{m_{o_{\text{LG}}}} + C_{m_{\alpha_{\text{LG}}}}\alpha\right)\delta_{\text{LG}} \end{aligned} \tag{14a}$$

$$\begin{aligned} C_n = {} & C_{n_o} + \left[C_{n_\beta} + C_{n_{\beta_{\text{LG}}}}\delta_{\text{LG}} + \Delta C_{n_\beta}(\delta_F)\right]\beta + C_{n_{\delta_r}}\delta_r + C_{n_{\delta_a}}\delta_a \\ & + \left[C_{n_{\delta_{\text{sp}}}} + \Delta C_{n_{\delta_{\text{sp}}}}(\delta_F)\right]\delta_{\text{sp}} + \left[C_{n_{r_s}} + \Delta C_{n_{r_s}}(\delta_F)\right](r_s b/2V) \\ & + C_{n_{p_s}}(\alpha)(p_s b/2V) + C_{n_{\delta_{\text{tr}}}}\delta_{\text{tr}} \end{aligned} \tag{14b}$$

$$\begin{aligned} C_l = {} & C_{l_o}(M) + \left[C_{l_\beta} + \Delta C_{l_\beta}(\delta_F)\right]\beta + C_{l_{\delta_r}}(\alpha)\delta_r \\ & + \left[C_{l_{\delta_a}} + \Delta C_{l_{\delta_a}}(\delta_F)\right]\delta_a + \left[C_{l_{\delta_{\text{sp}}}} + \Delta C_{l_{\delta_{\text{sp}}}}(\delta_F)\right]\delta_{\text{sp}} \\ & + \left[C_{l_{r_s}} + \Delta C_{l_{r_s}}(\delta_F)\right](r_s b/2V) \\ & + \left[C_{l_{p_s}}(\alpha) + \Delta C_{l_{p_s}}(\delta_F)\right](p_s b/2V) + C_{l_{\delta_{\text{tr}}}}(\alpha)\delta_{\text{tr}} \end{aligned} \tag{14c}$$

The coefficients are shown to contain functionality in Mach and angle of attack, as well as extended landing gear and flap setting effects.

As is often the case in aircraft system identification, several control surfaces lacked adequate excitation to facilitate successful extraction of their aerodynamic effects. Because of the lack of independent excitation for the horizontal stabilizer and rudder tab surfaces during the maneuvers, their effects were held constant at original OFT model values.[6] In addition, high correlation between aircraft angle-of-attack rate and body axis pitch rate required that aerodynamic coefficient effects by the former be fixed to original OFT values while effects of the latter were estimated.

The overall model identification process in Athena began with the initial definition of all force and moment aerodynamic model structures for the cruise configuration/gear up (CCGU) case. This model would be developed using the cruise flap setting/landing gear up analysis group in IDEAS. Each axis for the total force and moment aerodynamic coefficients reconstructed from flight data was examined separately using Athena. Initial model structures were as simple as possible, containing no functionalities for the aerodynamic stability derivatives. The resulting Athena fit percentage and Theil's fit statistics for these simple models were retained and used as a basis of comparison for future model structures. The functionality and/or structure of each total coefficient model was then methodically expanded and identified within Athena. Coefficient functionalities investigated were based on those expressed in the original OFT aerodynamic model, as well as those deemed plausible by experience. The final CCGU aerodynamic force and moment models were chosen as those with the best increase in Athena fit

percentage F and most favorable Theil's fit statistic information, U_b, U_v, and U_c.

The base aerodynamic force and moment models resulting from analysis of the CCGU case would act as a priori structures and values for the next analysis phase. From these base models, incremental aerodynamic effects due to various flap settings, as well as landing gear extension, would be estimated. The previously identified cruise force and moment aerodynamic models were frozen within Athena while the remaining analysis groups were examined. The four remaining PID maneuver groupings represented various flap configuration settings as well as landing gear deployment. Again, with the base cruise models frozen within Athena, the fit percentage and Theil's fit statistic information were recorded for the remaining analysis groups. Incremental effect coefficients were then methodically added to the frozen cruise model within Athena and estimated. These added terms modeled the effect of static flap position and/or extended landing gear on prominent coefficients currently existing in the CCGU Athena developed model. Again, the fit percentage and appropriate Theil's fit statistics were monitored to examine added coefficient increment effects on the fit quality. Similarly, flap and landing gear incremental effect coefficients investigated were based on structures expressed in the original OFT aerodynamic model, as well as those deemed plausible by experience.

As an overall example of this estimation process, consider the subcoefficient structure of the stability axis total rolling moment coefficient shown in Eq. (14c). The base CCGU aerodynamic model was found to contain a significant aerodynamic bias term, C_{l_o}, that varied with Mach. This was consistent with pilot comments regarding a persistent, and noticeable, aircraft left wing down rolloff required to be trimmed out for straight and level flight for this particular aircraft. All maneuvers recorded a significant level of aileron trim set by the flight crew to counter the left wing down tendency. Additional terms in the CCGU roll model include standard coefficients modeling the effects of pertinent control surfaces such as rudder, $C_{l_{\delta_r}}$, aileron, $C_{l_{\delta_a}}$, differential spoiler, $C_{l_{\delta_{\mathrm{sp}}}}$, and rudder trim tab, $C_{l_{\delta_{\mathrm{tr}}}}$. The remaining base model terms involve the dihedral effect, C_{l_β}, roll damping, $C_{l_{ps}}$, and the effect due to yaw rate $C_{l_{rs}}$.

To outline this analysis technique, consider the following rolling moment model development example. An analysis group of 18 lateral–directional PID maneuvers was examined during the development of the stability axis rolling moment coefficient cruise configuration model within Athena. The final model structure, as outlined in Eq. (14c), resulted in an Athena fit percentage F of 86.8% with fit error proportioned into 0% bias, U_b, 1.7% variance U_v, and 98.3% covariance, U_c, for the analysis group as a whole. This indicates the developed model does not contain systematic error and system variability is emulated with good accuracy. A sample history comparison between flight reconstructed and Athena model estimated stability axis total rolling moment coefficient is shown in Fig. 2 for a lateral stick doublet flown under cruise conditions.

The remaining four lateral–directional analysis groups were examined for rolling moment model development. No significant rolling moment effects were determined due to extended landing gear. However, because many of the rolling moment coefficients are strongly affected by wing lift and airflow distribution, particularly wing-mounted lateral control surfaces, significant incremental adjustments to the model were necessary when the extended flap configurations were examined. For example, as wing panel lift increases with flap deployment, incremental changes in the aileron and spoiler effectiveness, $\Delta C_{l_{\delta_a}}$ and $\Delta C_{l_{\delta_{\mathrm{sp}}}}$, were determined. In fact, flap deployment was found to increase aileron effectiveness overall with a maximum increase of 23.5% at takeoff setting, $\delta_F = 25$ deg, and trailed off to a 16.2% increase in landing configuration, $\delta_F = 35$ deg. Spoiler effectiveness followed an identical trend with a steady, and considerable, increase in effectiveness of 54.6% in takeoff and 43.8% in landing flap configurations, respectively. Similarly, a maximum 8.5% increase in roll damping ΔC_{l_p}, was found to occur in the takeoff flap configuration trailing off to a 4.9% increase in landing configuration. This increase in roll damping is as expected. C_{l_p} is primarily driven by increased lift generated by the downward-rotating wing as its local angle of attack is increased. This may also be the reason for the lower increase in roll damping at full flap deflection in that downward wing motion may reach a less effective relative angle of attack. The dihedral effect, ΔC_{l_β} and roll due to yaw rate, ΔC_{l_r} were enhanced by flap deflection with their greatest increases in magnitude of 7.1 and 11.6%, respectively, in landing flap configuration.

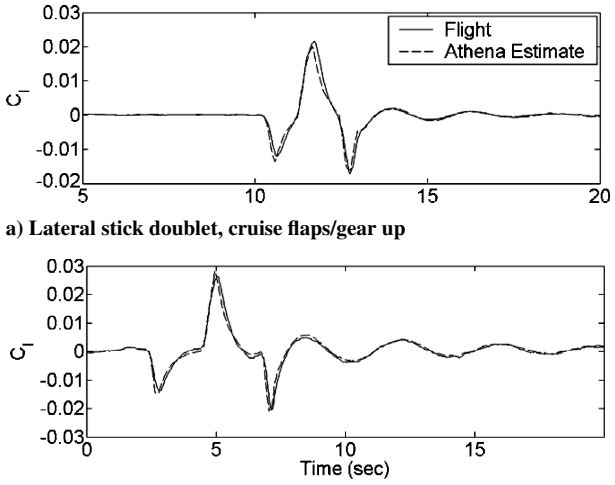

a) Lateral stick doublet, cruise flaps/gear up

b) Lateral stick doublet, landing flaps/gear down

Fig. 2 Comparisons between flight-reconstructed and Athena-estimated total stability axis rolling moment coefficients for cruise and landing configurations.

As an example of fit quality achieved with flaps deployed, consider the analysis group of six lateral–directional PID maneuvers in the landing flap, gear down configuration. The final Athena model structure incremental coefficients for rolling moment resulted in an Athena fit percentage F of 88.4% with fit error proportioned into 0% bias U_b, 0.8% variance U_v, and 99.2% covariance U_c for the group as a whole. A sample history comparison between the flight-reconstructed and the Athena model estimated stability axis total rolling moment coefficient may also be seen in Fig. 2 for a lateral stick doublet flown under landing flap, gear down conditions.

All total force and moment coefficients were studied in this manner and resulted in a new preliminary aerodynamic model for the S-3B. Because of any unidentified measurement errors among the independent variables, specifics in estimation technique such as holding parameters to available wind-tunnel estimates, and/or nonuniform distribution of the regressors, the parameters output by this estimation technique can be biased. Consequently, this new model was tuned with an output error estimation algorithm as discussed in the next section.

Model Adjustments Using Output Error

Estimation Algorithm

The output error optimization tool within IDEAS is the robust, adaptive nonlinear least-squares algorithm LSIDNT. LSIDNT is based on the N2F family of algorithms encompassing the Newton minimization scheme with an augmented version of the Gauss–Newton approximation (see Ref. 12). This algorithm works to minimize the standard least-squares cost function given a defined set of residuals to consider. This tool works in cooperation with a flight dynamics simulation hosted within the IDEAS environment.

Algorithm Application

Recall the equation error PID analysis of the preceding section resulted in an updated aerodynamic model for the S-3B. This upgraded model was installed in the S-3B nonlinear six-degree-of-freedom (DOF) simulation within IDEAS. The simulation could then be propagated by trimming to flight-recorded initial conditions and overriding appropriate recorded control deflections. These runs were performed on representative longitudinal, lateral, and directional PID maneuvers at different Mach, angle of attack, and landing gear/flap configurations. The resulting simulation output was

visually compared with flight data to deduce areas where the new model required adjustment, for example, monitored for deficiencies in damping, control authority, etc.

Overall, the Athena-generated model was found to be quite representative. However, some adjustments were necessary. Again, visual comparison between the new simulation output and calibrated flight data gave good clues as to what terms in the aerodynamic model required alteration. Final adjustments were made using the output error approach within IDEAS to estimate incremental coefficients applied to the existing Athena-generated model terms.

Unknown incremental variables were placed throughout the aerodynamic model which affected Athena-derived parameters under question within the new simulation. Consider an example where directional model characteristics were examined to uncover a need for changes in yaw damping, directional stability, and/or rudder control power. In this case, the following terms were added to the total aerodynamic yawing moment coefficient within the updated six-DOF simulation in IDEAS:

$$\Delta C_n(\beta) = \left(C_{n_{\beta_{\text{Athena}}}} + \Delta C_{n_{\beta_{\text{Out Err}}}}\right)\beta$$

$$\Delta C_n(r_s) = \left(C_{n_{r_{s_{\text{Athena}}}}} + \Delta C_{n_{r_{s_{\text{Out Err}}}}}\right)(r_s b/2V)$$

$$\Delta C_n(\delta_r) = \left(C_{n_{\delta_{r_{\text{Athena}}}}} + \Delta C_{n_{\delta_{r_{\text{Out Err}}}}}\right)\delta_r \qquad (15)$$

Individual lateral stick and rudder pedal input PID maneuvers were examined to investigate required incremental corrections to directional stability, ΔC_{n_β}, and yaw damping, $\Delta C_{n_{r_s}}$, coefficients. In addition, the rudder pedal input PID maneuvers also produced estimates for incremental corrections to rudder control power, $\Delta C_{n_{\delta_r}}$. Resulting coefficients from each analysis were plotted vs Mach with any trends noted. Because multiple maneuvers were flown at five distinct Mach points, the incremental output error estimates were averaged at each flight condition to yield the final estimates shown in Fig. 3. Figure 3 presents results for each directional correction in the form of the ratio of correction required to the original equation error estimate. This presents the output error results in the form of a relative change in magnitude allotted by the estimates. Recall from Eq. (14b) the original equation error estimate for directional stability C_{n_β} was constant throughout the flight envelope. However, Fig. 3 clearly indicates an increasing trend in directional stability, ΔC_{n_β} as Mach increases. This functionality was not uncovered during the equation error analysis. Figure 3 also indicates that a fairly constant increase in rudder control power, $\Delta C_{n_{\delta_r}}$, is required throughout the flight envelope and that a significant envelope wide constant decrease in yaw damping ($\Delta C_{n_{r_s}}$) is also required.

Additional model adjustment estimates were determined as appropriate for all axes in a similar fashion. Once the incremental estimates had been obtained, these adjustment parameters were applied to the Athena base model, resulting in the final extracted PID model. Of course, this model is valid for a certain region within the aircraft flight envelope. To obtain full envelope coverage, this model update was blended into the original S-3B OFT aerodynamic database to yield the proposed new model.

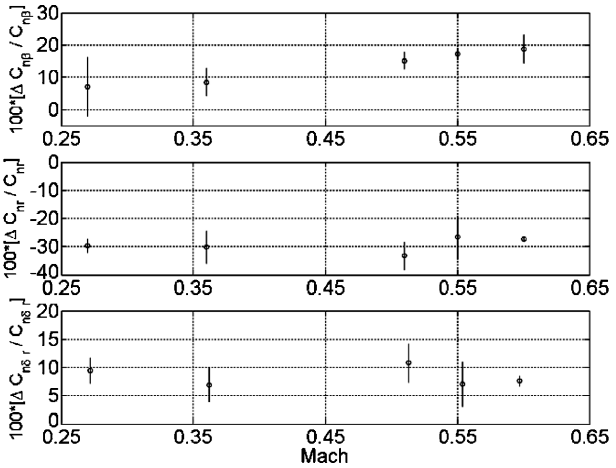

Fig. 3 Output error estimates indicating relative changes in magnitude of various yawing moment coefficients as a function of Mach.

Upgraded Simulation Validation

Sample response history plots comparing the SAIC-developed fully blended flight model with the original S-3B training simulation airframe model are shown in Figs. 4–6 for a longitudinal, directional, and lateral doublet maneuver compared with flight data. The baseline and updated model responses are a result of setting the aircraft loading and configuration in the simulation to match each PID maneuver, trimming the simulation, and propagating while overriding control surface deflections with flight-test signals. Each of Figs. 4–6 contains recorded flight data, original S-3B baseline, and SAIC-updated S-3B model response histories. This allows for an excellent comparison between the fidelity of both models. Marked improvement is evident in all axes for the updated model.

The longitudinal stick doublet response shown in Fig. 4 indicates higher fidelity in static trim for angle of attack. The longitudinal peak pitch rates are also captured more realistically in the updated simulation.

The directional pedal doublet maneuver of Fig. 5 shows an improvement in yaw axis damping and natural frequency during the transient response. Similarly, improvement is also found in roll axis damping and natural frequency. Capture of initial roll rate peaks has improved with the updated model.

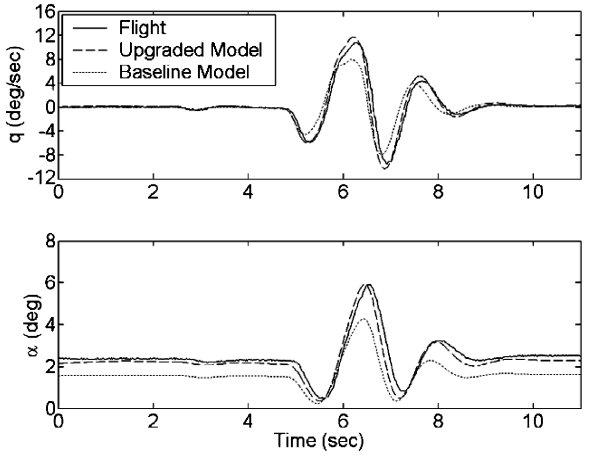

Fig. 4 Response history comparison between baseline and updated aerodynamic model with flight data for a longitudinal stick doublet.

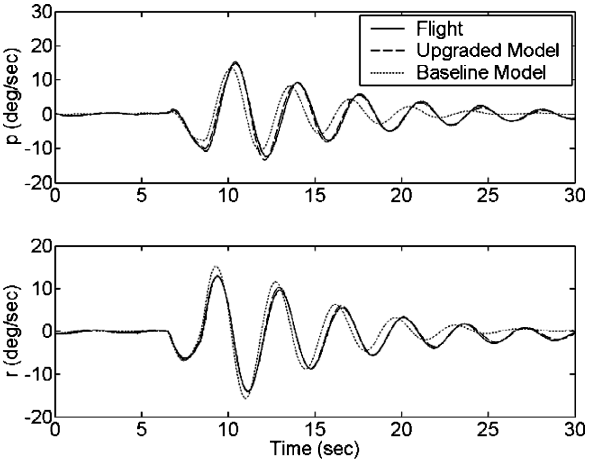

Fig. 5 Response history comparison between baseline and updated aerodynamic model with flight data for a directional pedal doublet.

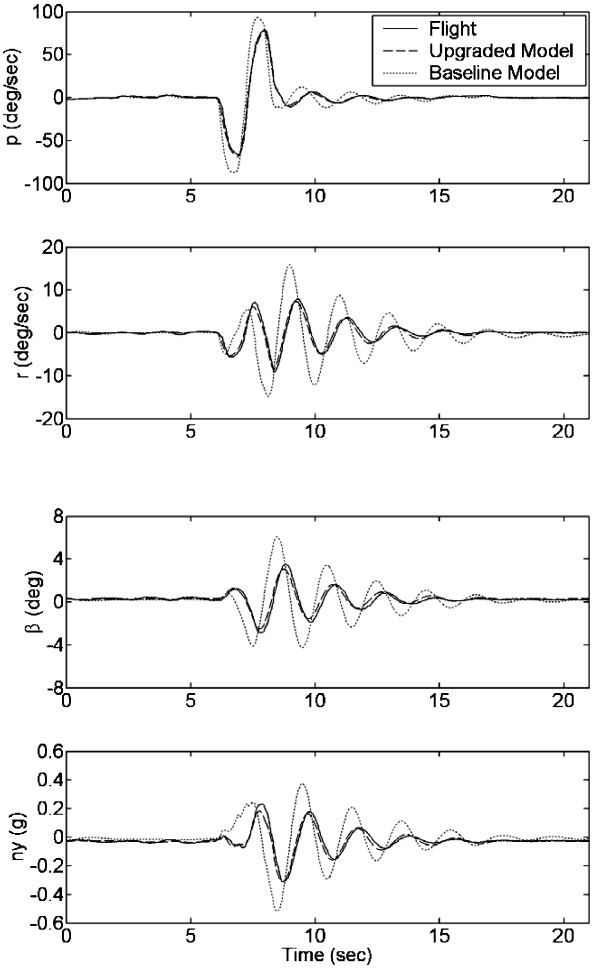

Fig. 6 Response history comparison between baseline and updated aerodynamic model with flight data for a lateral stick doublet.

The greatest increase in fidelity is shown by the lateral stick doublet maneuver of Fig. 6. The updated model produces an excellent match with recorded flight responses during the initial lateral control input as well as throughout the transient response. This can be said for both the primary roll axis and cross axis yaw responses.

Conclusions

A nonlinear aerodynamic model has been developed and installed within a nonlinear six-DOF simulation within IDEAS, for the S-3B Viking. Early model structure determination employed an equation error estimation algorithm. Final model adjustments were determined using an output error estimation technique. The entire process, from database management of the flight data, to validation of the proposed updated aerodynamic model, was completed within the IDEAS environment.

The SAIC-developed nonlinear aerodynamic model presents significant improvements in both longitudinal and lateral–directional characteristics including short period, Dutch roll modes, and control authority. These improvements result in potential simulation handling qualities much more representative of the true aircraft in both high and low gain flight tasks within the flight envelope where test data are available.

At present the updated simulation package has been installed in a development OFT device at a pilot training facility at North Island Naval Air Station. The updated OFT aerodynamic model is undergoing both pilot qualitative and engineering quantitative evaluation and validation studies in an effort toward final acceptance as an official training airframe.

References

[1]Alaverdi, O., "Analysis and Upgrade of Device 2F92B Aerodynamic Model Using Flight Data Collected During 1992 From S-3A BuNo 159736," Science Applications International Corp., SAIC Rept. 1393-2994-3, Lexington Park, MD, May 1995.

[2]Linse, D. J., "Aircraft System Identification Using Integrated Software Tools," *Proceedings of the RTA-SCI Symposium*, Systems Concepts and Integration Panel, Madrid, Spain, Paper No. 11, 5–7 May 1998.

[3]Linse, D. J., "Improving Simulator Accuracy With Integrated Analysis of Flight Data," Interservice/Industry Training, Simulation, and Education Conf., I/ITSEC Paper EC-046, Nov. 2000.

[4]Paris, A. C., and Alaverdi, O. "Post-Flight Inertial And Air-Data Sensor Calibration," AIAA Paper 98-4450, Aug. 1998.

[5]"NATOPS Flight Manual Navy Model S-3B Aircraft," U.S. Naval Air Systems Command, Rept., NAVAIR 01-S3AAB-1, Aug. 1996.

[6]S-3A Stability and Control Group Aerodynamics Department, "S-3A Aerodynamic Stability and Control and Flying Qualities Report," Lockheed Rept. 23462-3, Vol. 3, Rev. E, Dec. 1975.

[7]"Upgraded Mathematical Model Report for Device 2F92B," Science Applications International Corp., SAIC Rept. 01-1393-9226-E005, Lexington Park, MD, May 1999.

[8]"Upgraded Propulsion Model for S-3B Device 2F92B," Science Applications International, SAIC Rept. 1393-6296-D001, Lexington Park, MD, April 1999.

[9]Anderson, L. C., "Robust Parameter Identification for Nonlinear Systems Using a Principal Components Regression Algorithm," AIAA Paper 85-1766, Aug. 1985.

[10]Linse, D. J., "System Identification Software Design Document and User's Manual for the Integrated Data Evaluation and Analysis System (IDEAS)," Science Applications International Corp., SAIC Rept. 01-1393-2990-A005/A006, Lexington Park, MD, Nov. 1997.

[11]Pindyck, R. S., and Rubinfeld, D. L., *Econometric Models and Economic Forecasts*, 3rd ed., McGraw–Hill, New York, 1991, pp. 336–342.

[12]Dennis, J. E., Jr., Gay, D. M., and Welsch, R. E., "An Adaptive Nonlinear Least-Squares Algorithm," *ACM Transactions on Mathematical Software*, Vol. 7, No. 3, 1981, pp. 348–368.